Environmental Science and Pollution Research (2024) 31:20556–20567
https://doi.org/10.1007/s11356-024-32467-y

RESEARCH ARTICLE

Synthesis and characterization of TiO_2-based supported materials for industrial application and recovery in a pilot photocatalytic plant using chemometric approach

Nicolò Ghibaudo[1] · Maurizio Ferretti[1] · Entesar Al-Hetlani[2] · Metwally Madkour[3] · Mohamed O. Amin[2] · Stefano Alberti[1]

Received: 22 November 2023 / Accepted: 9 February 2024 / Published online: 20 February 2024

Abstract

In this contribution, the performance of powdered titanium dioxide (TiO_2)–based photocatalysts was evaluated in a pilot photocatalytic plant for the degradation of different dyes, with an investigated volume of 1 L and solar simulated light as irradiation source. Five different samples, synthesized in our laboratories, were tested in the pilot plant, each consisting of TiO_2 nanoparticles (NPs) coupled with a different material (persistent luminescent material and semiconductor material) and treated in different thermal conditions. All synthesized samples have been subjected to X-ray diffraction (XRD), X-ray photoelectron spectroscopy (XPS), Brunauer–Emmett–Teller analysis (BET), and transmission electron microscopy (TEM) characterization, to shed light on the influence of introducing other materials on titania characteristics. To study and evaluate the significance of the parameters affecting the process in the pilot plant, a chemometric approach was applied, by selecting a mathematical model (D-Optimal) to simultaneously monitor a large number of variables (i.e., 7), both qualitative and quantitative, over a wide range of levels. At the same time, the recovery of the synthesized photocatalysts was studied following a novel promising recuperation method, i.e., annulling the surface charge of the suspended samples by reaching the isoelectric point (pH_{PZC}) of each sample, for the quantitative precipitation of TiO_2 nanoparticles.

Keywords Heterogeneous photocatalysis · Chemometrics · Point of zero charge · Pilot plant · Enhanced sedimentation

Introduction

Water is undoubtedly a vital natural resource for mankind and for all ecosystems, and its preservation from the increasing consumption represents one of the main environmental challenges of the current century (Sousa et al. 2018). In addition, the constant replenishment of numerous chemical substances in water bodies is posing additional threats: These compounds, which have the potential to cause hostile effects

Responsible Editor: George Z. Kyzas

Highlights
- The number of experiments was reduced with D-Optimal chemometric approach.
- Functionalized TiO_2-based supported samples were synthesized and characterized.
- Samples were quantitively and rapidly recovered by annulling their surface charge.

✉ Stefano Alberti
stefano.alberti@unige.it

Nicolò Ghibaudo
nicolo.ghibaudo@edu.unige.it

Maurizio Ferretti
ferretti@chimica.unige.it

Entesar Al-Hetlani
entesar.alhetlani@ku.edu.kw

Metwally Madkour
metwally.madkour@sci.aru.edu.eg

Mohamed O. Amin
mohamed.amin@ku.edu.kw

[1] Chemistry and Industrial Chemistry Department, University of Genoa, Via Dodecaneso 31, 16146 Genoa (Ge), Italy

[2] Chemistry Department, Faculty of Science, Kuwait University, P.O. Box 5969, 13060 Safat, Kuwait

[3] Chemistry Department, Faculty of Science, Arish University, Al-Arish 45511, Egypt

on the environment and human health, are often collectively referred to as emerging contaminants (ECs) (Pal et al. 2010; Rykowska and Wasiak 2015). They include a wide range of different compounds, together with their degradation by-products, such as pharmaceuticals, personal care products, pesticides, veterinary products, and industrial additives (Alberti et al. 2021c; Yang et al. 2017). Such contaminants are characterized by a wide range of physical–chemical properties and very low concentrations (Ahmed et al. 2021; Dulio et al. 2018). Among the treatments designed for the removal of emerging pollutants, advanced oxidation processes (AOPs) are considered the most promising approach (Abdulrazaq et al. 2021; Deng and Zhao 2015; Dulio et al. 2018; Koumaki et al. 2015); an example is represented by heterogeneous photocatalysis, which is extensively studied to deal with ECs and their respective reaction intermediates (Ribeiro et al. 2015). Photocatalysis represents a unique class of reactions, where a semiconductor material, the photocatalyst, upon absorption of photons with a proper wavelength, exploits the energy absorbed from the light to carry out chemical reactions (Antonopoulou et al. 2021; Yang and Wang 2018). The photocatalytic process has several advantages, such as complete mineralization of pollutants, no chemical consumption, absence of waste disposal problem, low cost, and mild temperature and pressure conditions (Bhatkhande et al. 2002; Rueda-Marquez et al. 2020; Yang and Wang 2018; Younis and Kim 2020).

The number of publications dealing with "photocatalysis" or "photocatalyst" (according to Scopus) is nonetheless raising (Rueda-Marquez et al. 2020) due to the many weaknesses that still affect the photocatalytic process, including maximization of light absorption, shift to the visible region, minimization of charge carriers recombination, maximization of charge transfer at the interface, avoidance of nanoparticle dispersion, and enhancement of recovery. Many approaches were performed to investigate how to overcome these issues, like doping, coupling with co-catalysts, and using different materials as support (Alberti et al. 2019, 2021b; Antonopoulou et al. 2021; Bhatkhande et al. 2002; Liu et al. 2021; Martinelli et al. 2018; Rueda-Marquez et al. 2020; Sivaraman et al. 2022; Tayyab et al. 2022, 2023; 2024; Yang and Wang 2018; Younis and Kim 2020). Among materials proposed for water decontamination, semiconductors like zinc oxide (ZnO) and TiO_2 represent the most popular options. A great advantage is represented by the synthetic process, as TiO_2 can be easily obtained through a soft chemistry synthetic route, e.g., sol–gel technique, which exploits mild temperature and pressure conditions and consequently a very low energy consumption. Furthermore, this synthetic approach allows an easy coupling with different types of innovative materials to endow the composite sample with additional features (Azeez et al. 2018; Bhatkhande et al. 2002; Sivaraman et al. 2022; Younis and Kim 2020). In this regard, it is has been recently documented how the photocatalyst supported on persistent luminescence materials (PeL) increased the overall efficiency and allowed the photocatalytic process to occur in the dark (Alberti et al. 2023; Azeez et al. 2018; Villa et al. 2016), which is significant in terms of reduction of energy consumption (Koumaki et al. 2015).

One of the major drawbacks related to the industrial use of photocatalysis is the difficulty to separate and recover the suspended photocatalyst after completing the water treatment process (Al-Hetlani et al. 2017). Different methods have already been proposed, such as the use of coagulants, ultrasonic radiation, or microfiltration, but they are expensive, often requiring special processes and/or the consumption of chemicals which may not be available to everyone. Nevertheless, there is still a strong need to establish alternative and simpler methods that can be appropriate for all types of nanosized photocatalysts (Umh and Kim 2014). One feasible example is represented by tailoring the surface charge of photocatalysts by adjusting the pH of the solution to reach the isoelectric point (pH_{IEP}), or point of zero charge (pH_{PZC}), where nanoparticles' suspension becomes unstable due to the lack of electrostatic repulsion; hence, a rapid sedimentation of the photocatalyst occurs. In particular, pH_{PZC} is the pH value at which the surface charge of the NPs is equal to zero, while above and below the pH_{PZC}, the nanoparticles possess a surface charge, which creates repulsion and maintain their colloidal stability as a suspension. Once the nanoparticles sedimented they can be easily separated, washed, and recycled again for more photocatalytic experiments. This should greatly reduce the amount of nanoparticles produced and consumed for future photocatalytic experiments (Al-Hetlani et al. 2017; Azeez et al. 2018).

In the present work, some of the major drawbacks related to the exploitation of heterogeneous photocatalysis were addressed and discussed. The prepared TiO_2-based nanoparticles were characterized by means of several physicochemical techniques (XRD, XPS, BET, TEM) to retrieve information on the influence of the coupling materials on the semiconductor. A photocatalytic pilot plant was set up, to simulate an industrial process exploiting heterogeneous photocatalysis for the degradation of emerging contaminants. A chemometric approach was applied to the photocatalytic tests performed with the pilot plant, to mathematically find out which significant variables should be controlled; these tests also included the assessment on the efficiency of five different synthetic photocatalysts. Eventually, an innovative recovery technique was tested with investigated samples, in order find out their pH_{ZPC}, to avoid their dispersion and consequently allow their reuse in such pilot plants. To the best of our knowledge, the application of a chemometric approach to a photocatalytic pilot plant has never been reported so far, while the number of papers dealing with chemometrics for photocatalytic experiments is still very limited and only

dealing with a small number of variables (Ba-Abbad et al. 2017; Boutra et al. 2022; Deriase et al. 2021).

Materials and methods

Chemicals

All descriptions of used reagents and materials are reported in SI.

Photocatalyst synthesis

In the present work, five different TiO_2-based photocatalysts were synthesized and investigated, and their synthetic conditions are summarized in Table 1 and reported below.

Each sample containing TiO_2 was prepared according to the following synthetic procedure: The sol–gel process was performed using TTIP, i-PrOH and H_2O in two different volume ratios, 1:2:5 and 1:34:5, respectively. TTIP and i-PrOH were mixed in an Erlenmeyer flask, to get a homogeneous solution. After a short time, water was quantitatively added and instantly the formation of the sol occurred. The solution was left under magnetic stirring for 4 h, to trigger the formation of the amorphous TiO_2 gel, for both volume ratios. Subsequently, the crystallization of TiO_2 was performed according to two different thermal treatments: a hydrothermal synthesis, carried out for 3 h at 150 °C in a Teflon reactor, filled to the half of the volume with the gel and immersed in a silicone oil bath; and a solid-state treatment, performed in a muffle furnace for 1 h at 350 °C on the powdered TiO_2, in turn obtained by drying the gel in an oven for 24 h at 105 °C and grinding it in an agate mortar. The PeL material was obtained by mixing ZnO, Ga_2O_3, GeO_2, and Cr_2O_3 in an agate mortar at a specific molar ratio (3:1:2) and then treated in the muffle furnace at 900 °C for 2 h and then at 1100 °C for additional 2 h. Eventually, ZnO was synthesized according to the nitrate-route, as previously described in Alberti et al. (2021a).

Physico-chemical characterization

All physico-chemical characterization techniques exploited in the present work are reported in SI.

Pilot photocatalytic plant

The pilot plant was studied and designed as tertiary module, to be put downstream of primary and secondary processes in WWTPs, specifically to face the problem of emerging pollutants. Different works reported in literature show different models of pilot plants (González-Pereyra et al. 2022; Merino-Mantilla et al. 2019); among the proposed ones, the most suitable was identified as the compound parabolic collector (CPC) solar photo-reactor (González-Pereyra et al. 2022; Sousa et al. 2012) which presents advantageous light-gathering properties and well-known design methodology (Luna-Sanguino et al. 2020). The prototype, shown in Figure S1, consists of a 1 L reactor (A), placed above a magnetic plate (B), and subjected to vigorous magnetic stirring. The container has an output connected to a pumping system (peristaltic pump, C), which allows the solution to flow continuously (max 1 L/min) in a glass coil (D), in which the solution can slide below the solar simulators. The coil, with a reduced diameter, is located above a tilting plane (E), covered in aluminum foil, and it ends up in the initial reservoir, to close the loop. This prototype cannot be exactly defined as CPC, but its design can be easily varied to adapt it, for example, changing the tilting plane below the glass coil. The solar radiation was simulated with two solar simulated light lamps (OSRAM ULTRA-Vitalux, 300W) placed at 20 cm above the coil.

Chemometric approach (D-Optimal)

The study of heterogeneous photocatalysis as oxidation process for the abatement of emerging pollutants in a real plant is quite demanding; hence, it was decided to apply a chemometric approach to this study, selecting a proper mathematical

Table 1 Summary conditions of synthesized samples

Sample	*Composition*	*Synthesis*	*Thermal treatment conditions*
S1	TiO_2	Gel (1:34:5)*	Hydrothermal treatment (3 h, 150 °C) Oven drying (24 h, 105 °C)
S2	TiO_2/PeL	Gel (1:34:5)* 75% TiO_2 gel + 0.5 g PeL	Hydrothermal treatment (6 h, 100 °C) Oven drying (24 h, 105 °C)
S3	TiO_2	Gel (1:2:5)*	Oven drying (24 h, 105 °C) Solid-state treatment (1 h, 350 °C)
S4	TiO_2/PeL	Gel (1:2:5)* TiO_2/Pel (1:1)#	
S5	TiO_2/ZnO/PeL	Gel (1:2:5)* TiO_2/ZnO/PeL (1:1:2)#	

*(V/V)

#(w/w)

model of experimental design compatible with numerous variables of both qualitative and quantitative nature. The design of choice was the D-Optimal, as it is the most suitable design, with respect to other models, to simultaneously manage a large number of variables (7) on a wide range of levels (which correspond to the different values of quantitative variables as well as different configurations of qualitative variables). The aim is to obtain information on the significance of each investigated variable and to evaluate any possible interactions occurring among variables. The D-Optimal model is described by a fundamental equation (Eq. 1), where the response Y is associated to each investigated variable (X_n) and their respective significance coefficient (b_n), together with the possible interactions terms (X_nX_m), and the respective interaction coefficients (b_{nm}).

$$Y = b_0 + b_1X_1 + b_2X_2 + b_3X_3 + b_4X_4 + b_5X_5 + b_{6A}X_{6A} + b_{6B}X_{6B} + b_{7A}X_{7A} + b_{7B}X_{7B} + b_{7C}X_{7C} + b_{7D}X_{7D} + b_{12}X_1X_2 + b_{13}X_1X_3 + b_{14}X_1X_4 + b_{15}X_1X_5 + b_{23}X_2X_3 + b_{24}X_2X_4 + b_{25}X_2X_5 + b_{34}X_3X_4 + b_{35}X_3X_5 + b_{45}X_4X_5 + b_{11}X_1^2 + b_{22}X_2^2 + b_{33}X_3^2 \quad (1)$$

The photocatalytic efficiency of the five synthesized samples was tested, in different experimental conditions, using MB, RhB, and MO as model pollutants, monitoring the decrease in absorbance by means of UV–Vis spectrophotometry as a function of time. The other variables monitored within this work were the pH of the solution, the concentration of the photocatalyst, the duration of the experiment, the position of the lamps, and the stirring speed of the solution.

The whole experimental domain investigated by the model is described by the chosen variables and the respective levels, reported in Table S1.

Experimental results are finally elaborated according to Eq. 1 using the coefficients obtained with a program able to compute the experimental design model (Chemometric Agile Tool; CAT) as reported elsewhere (Leardi et al. 2019). One of the main advantages in using this model is that the whole number of experiments is firstly calculated by CAT software, according to the defined experimental domain (considering all possible combinations of our investigated variables and their respective levels, the total number should be 1620). Having this set of candidate points, by the study the factors' covariance, which indicates the degree of correlation between one variable and another, the mathematical model suggests then the minimum number of experiments required to get the most comprehensive information out of the experimental domain. This specific information is retrieved by studying the maximum inflation factor (MIF) as a function of the number of experiments, which should be equal to or less than 4, to be considered as acceptable (Benedetti et al. 2023). As an example, the factors' covariance, represented with the MIF index, as a function of the number of experiments is reported in Fig. S2. In order to increase the covariance and thus decrease MIF to a value lower than 1, the final number of experiments was selected as 32. Experiments to be performed were randomly chosen by the program out of the 1620 possible experiments. Each experiment was performed to retrieve the final abatement degree of the model pollutant which is the response "Y" to be maximized in Eq. 1.

Photodegradation experiments

All the experiments performed are carried out to retrieve the efficiency of the synthesized samples in different experimental conditions, as summarized in Table S1. The mathematical model helps to understand the significance of the chosen variables and possible interaction among variables which may enhance/decrease the efficiency. In order to do this, the dye solutions were subjected to photocatalytic tests and the abatement degree (Eq. 2) was calculated as a function of time of the experiment, followed by taking aliquots at fixed times, as follows:

$$Abb\%(t) = \left[\frac{C_0 - C_t}{C_0}\right] \times 100 \quad (2)$$

where $Abb\%(t)$ represents the abatement degree for each time "t" corresponding to the time of aliquot withdrawal, calculated by means of the initial concentration "C_0," corresponding to 10 mg L^{-1}, and the concentration of the dye along time "C_t." The dye concentration was calculated according to a calibration line performed prior to each experiment, thanks to the Beer-Lambert law. Quantitative measurements were performed with a Lambda 35 UV–Vis spectrophotometer (PerkinElmer), monitoring the absorbance at wavelengths of 664.6 nm, 464.4 nm, and 553.8 nm for MB, RhB, and MO, respectively.

Recovery at pH_{ZPC}

The possibility to quantitatively recover the suspended photocatalysts from the aqueous solutions treated in the proposed pilot plant was investigated by studying the point of zero charge of each sample. In fact, by adjusting the pH of the aqueous solution, it is possible to study the change in the Z-potential (ζ) value, which is related to the surface charge of the photocatalyst, to find the pH conditions for which the Z-potential becomes equal to 0. This is the condition known as point of zero charge, or isoelectric point, respectively reported as pH_{PZC} or pH_{IEP}. ζ measurements were carried

out using a Zeta sizer Nano ZS (Malvern Instruments Ltd, Malvern, UK). The measured electrophoretic mobilities were converted to ζ-potentials using Dispersion Technology Software (version 5.03, Malvern Instruments Ltd., UK). Once pH_{ZPC} was found, sedimentation experiments were carried out with a Turbidimeter (Turb 550, WTW, Germany) to measure the recovery rate. Samples were suspended in water (1 g/L), at the isoelectric point (pH_{IEP}), and the sedimentation behavior of the samples was investigated as a function of time, by following the change in turbidity of the suspension, measure in nephelometric turbidity units (NTU).

Results and discussion

Characterization results

Different physico-chemical characterizations were employed to analyze the synthesized samples, to investigate their morpho-structural properties and define the correlation between the composite's features and the displayed efficiency.

Figure 1 shows the XRD patterns obtained for all synthesized samples, together with anatase TiO_2 reference pattern, retrieved from Pearson's Crystal Data database, and bare PeL XRD pattern, used as reference for the PeL material.

The XRD analysis revealed the presence of the main phase of TiO_2, i.e., anatase crystalline phase, visible in all samples. In particular, S1 (black line) shows only anatase phase peaks (as it is possible to assume by the comparison with the reference pattern (dark gray bars)) in the typical form of nanoparticles for the full width at half maximum of the peaks, attributable to the small dimension of the crystallites (also according to Scherrer equation, where the FWHM is inversely proportional to the crystallite's size). S3 (wine line), analogously, shows diffraction peaks ascribable to the anatase phase, while an extra peak, centered at 30°, is the proof that the thermal treatment employed leads also to the formation of brookite as secondary phase (since only the main peak is visible in the pattern, it can be assumed that it is present in a very small amount). Supported samples, that are S2 (red line) and S4 (blue line), present both contributions of TiO_2 and PeL to the patterns; at first sight, S4 seems to be slightly different in terms of weight percentage of each component, as S2 has more intense TiO_2 peaks, while S4, conversely, has more intense PeL peaks. This must be attributed to the synthetic procedure employed. S5 (green line), which is a three-component supported sample, mainly shows the PeL pattern, as it is possible to notice by comparing with the PeL reference, while TiO_2 presence is just touched upon. ZnO pattern (Alberti et al. 2021a) results instead to be not visible, mainly because it is also a component of the PeL material (as anticipated in the "Photocatalyst synthesis" section); thus, its presence in S5 sample is hidden by the PeL reference.

The morphology of the synthesized TiO_2 NPs at different temperatures with and without hydrothermal treatment was

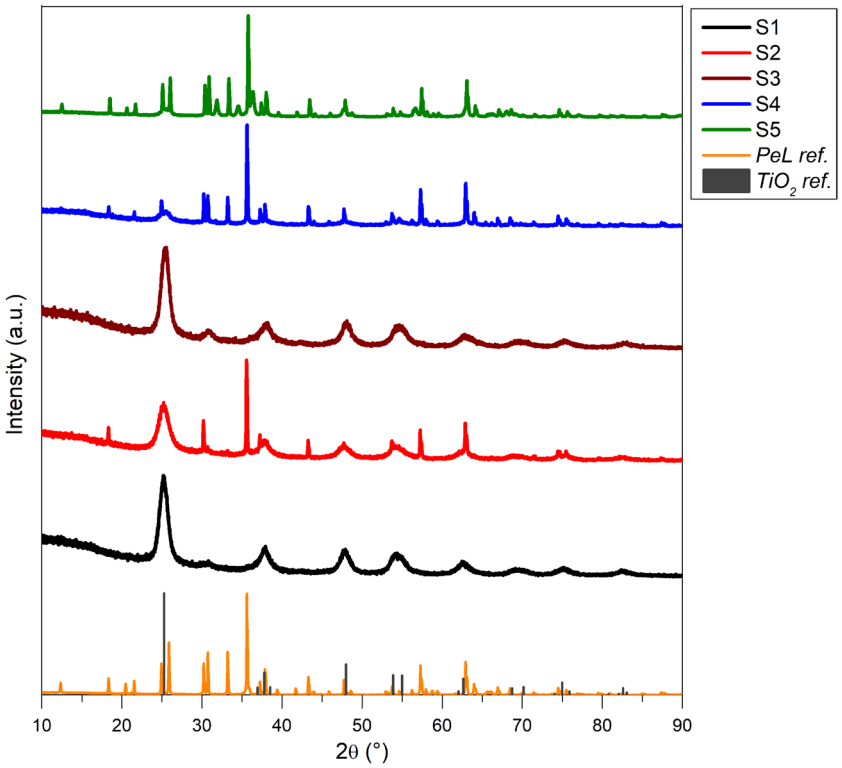

Fig. 1 XRD normalized patterns of all samples and anatase TiO_2 and PeL references

investigated via transmission electron microscope (TEM) as shown in Fig. 2. All samples revealed a semispherical irregular shape. The irregular morphology of TiO_2 NPs was a consequence of the lack of steric stabilization exerted on the titanium cores before they agglomerate to form the TiO_2 NPs. As the preparation temperature increased, the particle size slightly increased (with particle size from 5.6 to 13.5 nm from sample S1 to S5). The sample TiO_2/ZnO/PeL (S5) revealed an improved dispersion compared to the other samples, and this is most likely attributed to the presence of PeL and solid-state treatment.

To confirm the surface composition and oxidation state(s) of the prepared TiO_2 NPs, X-ray photoelectron spectroscopic study (XPS) was performed and the results are shown in Fig. 3. The surface oxygen (O 1 s spectrum) is attributed to O^{2-} species in TiO_2 (B.E. = 529.9 eV); a small peak appears at 531.2 eV and is assigned to OH − (surface hydroxyl) (Vasilopoulou 2014). The binding energies of Ti $2p_{3/2}$ and Ti $2p_{1/2}$ are observed approximately at 458.9 and 464.4 eV, respectively (Grbić et al. 2014). The ratio of the areas of the two peaks $A(\text{Ti } 2p_{1/2})/A(\text{Ti } 2p_{3/2})$ is equal to 0.4, and the binding energy difference due to the spin–orbital coupling, $\Delta E_b = E_b(\text{Ti } 2p_{1/2}) - E_b(\text{Ti } 2p_{3/2})$, was 5.7 eV in good agreement with the expected and reported value.

The porous structure of the prepared nanoparticles was investigated using nitrogen adsorption and desorption isotherms measured at 77 K, as shown in Fig. 4. All samples can be classed as type IV, which indicates the mesoporous nature of the prepared materials (as demonstrated in Table 2). For S1 sample, the adsorption isotherm can be classified as H3, whereas S2–S5 had a hysteresis shape between H1 and H3 (Thommes et al. 2015). The adsorption outlet S1 showed a significant increase at low pressure (< 0.01 P/P_0), whereas S2–S5 exhibited a lower adsorption, the BET surface area

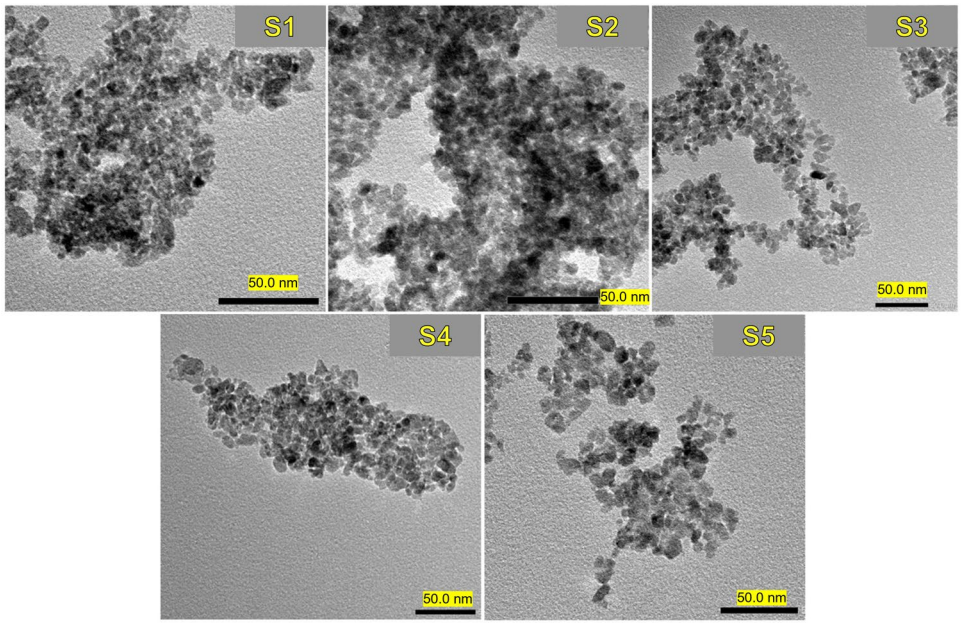

Fig. 2 TEM images of the five different TiO_2-based photocatalysts employed in the present work (for each image, the black marker is referred to 50 nm length)

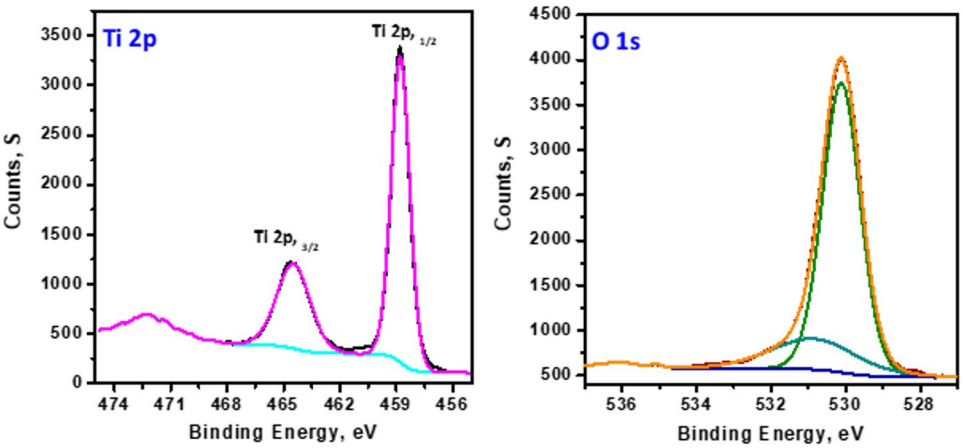

Fig. 3 XPS of S1 sample, Ti 2p, and O 1 s spectra

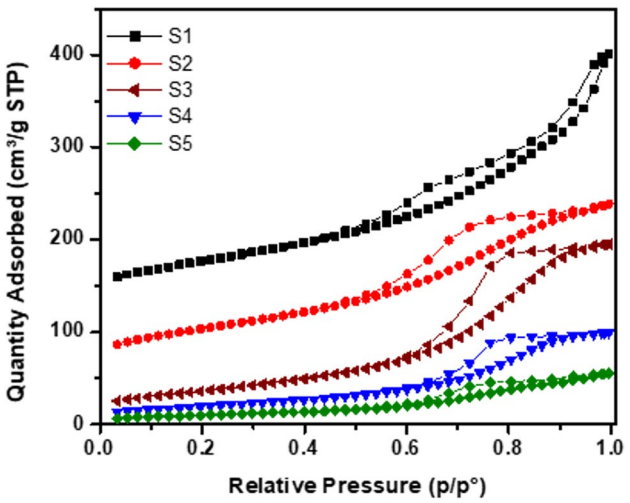

Fig. 4 N_2 adsorption isotherms of the five different TiO_2-based photocatalysts employed

Table 2 Pore size (nm), pore volume (cm^3/g), and BET surface area of the NPs

Sample	Pore size (nm)	Pore volume (cm^3/g)	BET surface area (m^2/g)
S1	9.04	0.43	189.22
S2	5.98	0.29	195.00
S3	9.20	0.30	131.09
S4	8.70	0.15	71.00
S5	9.43	0.09	36.70

of 189.22 $m^2\ g^{-1}$ was obtained for S1 followed by a slightly higher surface area for S2 (195.00), and then, a decrease in surface area was measured at 131.09, 71.00, and 36.70 $m^2\ g^{-1}$ for S3, S4, and S5, respectively. The high surface area values found for S1 and S2 can be safely attributed to the hydrothermal treatment employed during the synthesis; the presence of the PeL material did not affect this value. This could be due to the high oven temperature used for drying and the solid-state treatment at 350 °C.

Photodegradation experiments according to the D-Optimal chemometric approach

Once the number of experiments was selected to be 32, as described in the "Chemometric approach (D-Optimal)" section, photocatalytic tests were carried out according to the levels of each variable indicated by the model. Table S2 reports the experimental conditions selected for each performed experiments by the CAT software.

Figure 5 shows the abatement degree calculated for all 32 experiments, in order to use the Abb% value as Y, obtained with the different X_n, in Eq. 1. For clarity, it was decided to merge all experiments performed using the same photocatalyst by reporting them under the same color.

At this point, the model can be processed, and consequently, the significance graph, the values of the "b_n" coefficients, and the response surfaces can be derived. By means of CAT program, once the final abatement values of each experiment have been entered, it is possible to solve the equation (Eq. 1) and assign a mathematical value to the "b_n"

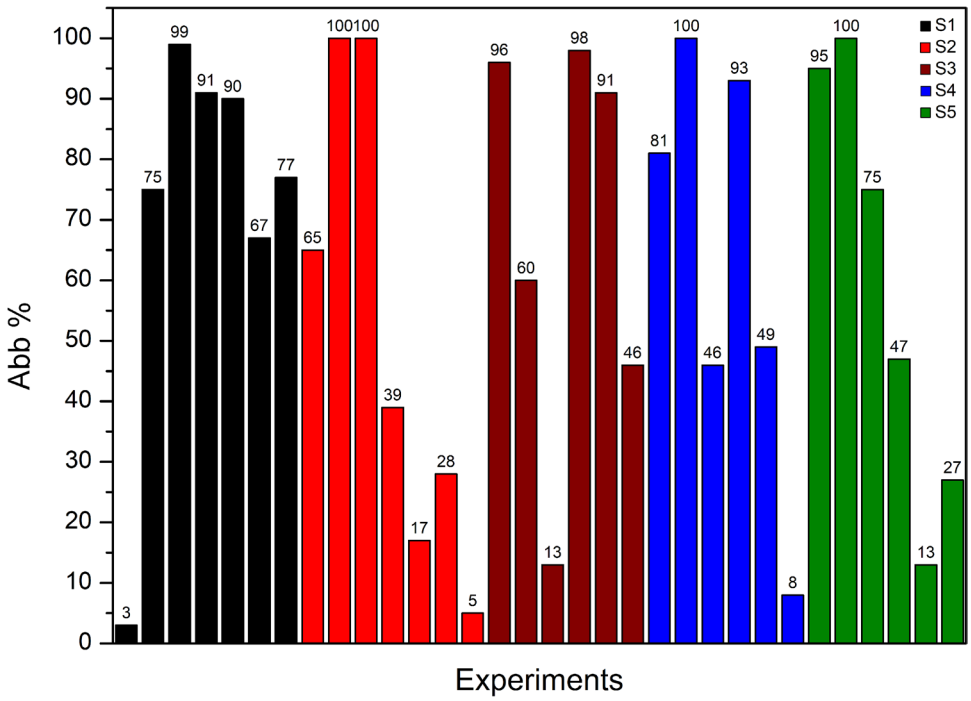

Fig. 5 Experimental results obtained as Abb% degree for all performed experiments

coefficients, reported as a graph (Figure S3). Each coefficient is reported with an error bar, which defines the significance of each coefficient by reporting different p values, namely, $*p<0.05$, $**p<0.01$, and $***p<0.001$.

From the graph, it is possible to determine which experimental variables were found to be important and therefore necessary to be highlighted: only 4 out of 25 coefficients were mathematically significant, respectively related to the following variables: X_3 (experiment duration), X_{6a} and X_{6b} (MB and RhB dyes), and $X_3 \times X_4$ (interaction term between experiment duration and lamp position variables).

Consequently, the other coefficients and their related variables resulted to be not significant to increase the percentage abatement of the investigated pollutants; indeed, their absolute values were lower than the corresponding standard deviations. Focusing exclusively on the significant variables, we can see that the time (X_3) has a positive coefficient, and this means that, within the experimental domain, a longer treatment time leads always to a higher percentage abatement. Therefore, increasing the treatment time when dealing with industrial pilot plants (designed as the one employed in this project) is a factor that must be considered. The other significant variables with a positive effect are X_{6a} and X_{6b}, corresponding to the use of MB and RhB. Being qualitative variables, the information that we can retrieve with the model is that basically the photocatalytic samples can effectively interact and degrade these two specific pollutants, likely due to electrostatic interaction with samples' surface or due to the molecular structure of the dye, which is easier to be degraded by photocatalytic reactions. This practically intends that some pollutants can be easily degraded in such pilot plant, while others can be more recalcitrant to photocatalytic degradation.

Unexpectedly, the product $X_3 \times X_4$ was also found to be significant, and for this reason, it was decided to report the response surface of these two variables to have a clearer vision (Fig. 6).

Figure 6a shows the relationship between time (X_3) and lamp position (X_4) variables, further underlined with the contour plot reported in Fig. 6b, which is a plane section of the response surface reporting the isolines of percentage abatement. The color scale on the right of Fig. 6a shows the response values (Abb%) ranging from 45% (yellow) to 100% (blue). It can be seen that a longer treatment time will lead to a higher dye degradation, as already mentioned above, but the additional information derived from the model is the interaction of this variable with the lamp positions, meaning that it is still also possible to obtain a high percentage of abatement with short time experiment simply by setting the solar lamps in a specific configuration (in our case, one lamp set above the coil and one above the container). This information can be thought of as practical hint for industrial photocatalytic plants, where time can be saved whether the irradiation with solar light is maximized in terms of exposed area.

Material recovery

An important factor that must be addressed when dealing with photocatalytic pilot plant is the recovery of the

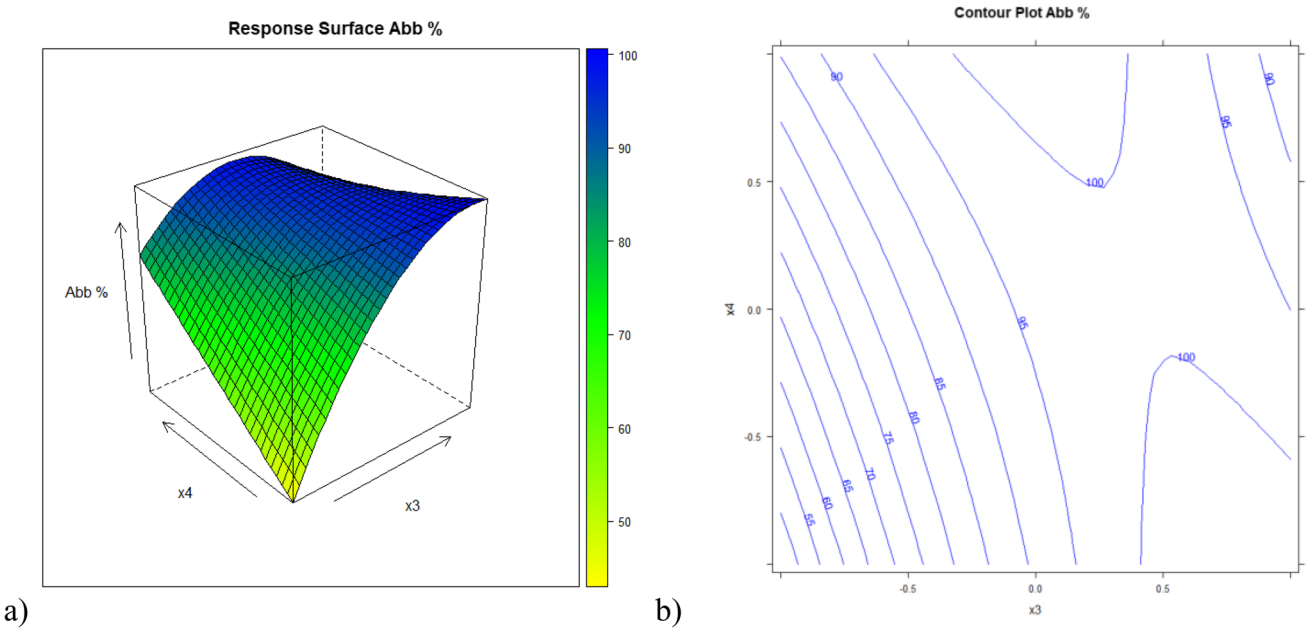

Fig. 6 **a**) Response surface of X_n variables "lamp position X_4 vs. experiment duration X_3"; **b**) contour plot

suspended photocatalyst. In general, the recovery of nanoparticles can be challenging, as the possibility to use filters or centrifugation is strongly hindered by the small dimensions of the particles and the huge volume of solution that should be treated in pilot plants can impede the exploitation of such procedures.

For this reason, as preliminary attempt, a sedimentation test by gravity with the aid of an Imhoff cone was performed and subsequent recycle tests were carried out to investigate the reusability of the photocatalyst. MO degradation tests were performed with S1, repeated over seven consecutive cycles: S1 was dispersed in 500 mL of 20 mg L^{-1} MO aqueous solution and left treating for 5 h; at the end of the experiment, the whole dispersion was transferred to the Imhoff cone and was left settling down for 4 days. After the 4-day sedimentation, the supernatant was withdrawn leaving behind the smallest volume of solution (50–100 mL), still with the settled photocatalyst. This volume was then added to a fresh MO solution, to carry on with the recycling tests. It must be underlined that the sample was not collected, washed, and dried until the last cycle, where it was finally quantified by weighing it. Experimental results shown a 40% efficiency loss, passing from 98.7 to 60.2% at the end of the first and at the end of the seventh cycle, respectively. As anticipated, only after the end of the last cycle, the remaining solution was dried in an oven at 105 °C for 24 h to weigh the remaining amount of sample. As a result, only 50% of the initial sample was retained. Thus, it can be safely assumed that the efficiency loss can be due to sample loss, which proportionally lead to a decrease in the MO percentage abatement as the catalyst's concentration decreased considerably (approximately 5% loss during each cycle). Furthermore, it is possible to suppose that the sample's losses occurred between each consecutive cycle were due to the lack of control in the sedimentation tests, so that a part of the suspended sample did not undergo natural sedimentation and was then washed away with the supernatant.

In order to avoid the loss of nanoparticles and the subsequent loss in efficiency, it was crucial to investigate an innovative recovery technique for all samples. Prior to the recovery test, which gives insights into the possibility to safely employ powdered photocatalysts in water treatment plants, the pH_{PZC} was studied for all samples; results are shown in Table 3.

We can see that some samples show more than one isoelectric point, and this is due to the existence in the supported samples of multiple materials other than titania showing different pH_{PZC} values.

The sedimentation behavior of the NPs was then recorded in terms of efficiency over time, as illustrated in Figure S4, and results are then summarized in Table 4.

Among tested samples, S5 resulted the fastest to be recovered at the highest efficiency, even though the same considerations may be done for all the other samples but S2. Results are promising, especially for the possibility of quantitative recovery of each sample at mild pH_{PZC} values. This outcome reflects how the exploitation of this recovery approach would highly enhance the retrieval of the photocatalysts used in water treatment plants and improve their safety, by impeding the loss of sample during multiple cycles.

Table 3 pH_{PZC} values found for tested powder samples

Sample	pH_{PZC}	Remarks
S1	5.77	-
S2	7.37	-
S3	8.19	-
S4	5.31	Sedimentation test performed at 6.29
	6.29	
	6.78	
S5	5.11	Sedimentation test performed at 5.98
	5.98	
	7.67	

Conclusions

A multivariate chemometric approach was successfully applied to the case study of a scalable and home-made heterogeneous photocatalytic plant based on a CPC design, which is reported to be one the best design choices among others for big water treatment facilities (Grčić et al. 2024; Mustafa et al. 2023; Rapti et al. 2023). Particularly, the application of the D-Optimal design helped to dramatically reduce the number of experiments while simultaneously evaluating the significance of each variable as well as exploring the possible interaction between them, which would not be possible with a mono-variate approach. Owing to its application, it was possible to recognize that, in such processes, some variables are more significant than others (type of pollutant, experiment duration, and interaction between time and lamp positions); hence, during an industrial scale-up, they should be carefully monitored and controlled. It is to be noted that the literature reporting the application of a chemometric model for such purposes is very scarce so far (Ba-Abbad et al. 2017; Boutra et al. 2022; Deriase et al. 2021); thus, we can assume that its exploitation may help in dealing with the same research problems.

All synthesized samples were proved to be mainly composed of anatase phase of TiO_2, even though S3 shown the presence of a small amount of secondary brookite, with dimensions lower than 10 nm, as disclosed by TEM. Surface area was recorded to be very high for the samples treated with hydrothermal process and with a higher isopropanol

Table 4 Recovery efficiencies (%) and time for complete sedimentation

Sample	Efficiency (%)	Time ($\times 10^3$ s)	Remarks
S1	97.6	88.7	Complete sedimentation after 1 day
S2	85.1	175	Complete sedimentation after 2 days
S3	97.3	88.7	Complete sedimentation after 1 day
S4	93.3	88.7	Complete sedimentation after 1 day
S5	99.3	88.7	Complete sedimentation after 1 day

volume during sol–gel synthesis (S1 and S2). To the best of our knowledge, we can state that no composite materials relying on the coupling between a semiconductor and a luminescent material was ever studied in a photocatalytic plant, as recent reports only discuss about commercial TiO_2 or general semiconductors fixed on solid supports (Chaubey et al. 2023; Grčić et al. 2024; Mustafa et al. 2023). Moreover, the sol–gel synthesis could be the right choice to maintain good levels of reproducibility, control over the purity, and morphology while scaling up towards a large-scale production. The hydrothermal heat-treatment should be also taken into consideration, but this would potentially become the bottleneck for the industrial production.

In addition, we focused on powdered composite materials thanks to the innovative method that we proposed for their recovery from aqueous suspensions. According to the most recent literature, there are some issues that should be still addressed while considering the practical application of photocatalysis on an industrial scale (Kuspanov et al. 2023), like the development of highly efficient photocatalysts with recycling possibility and minimal loss of photocatalytic activity. The immobilization of the photocatalyst on a solid base seems to be the most suitable option, but the reduction in exposed surface area is often proportional to the reduction of photoactivity. Hence, the possibility to recover the suspended NPs by reaching the isoelectric point would help in principle to avoid the need of solid supporting materials and let the whole exploitation of NPs' potential.

S1 could be recycled for at least seven cycles, but the unattended recovery by sedimentation led to a decrease in efficiency of ca. 40%, which was imputed to the material loss. Additionally, the sedimentation took place for 4 days between each consecutive cycle. Among all samples, S2 resulted to be the slowest to be recovered while S5 the fastest. As the type of sample was not significant according to the chemometric outcome, it is possible to opt for the sample which is recovered faster, to further save time and decisively apply this kind of technology in actual treatment plants. The proposed approach was investigated to prove that the isoelectric point can allow the full recovery of the suspended photocatalysts, ensuring maximum efficiency in consecutive cycles.

Future developments may include the chemometric study of our synthesized photocatalysts in the pilot plant against real pollutants and in increasing treating volumes, carrying out a comprehensive study on the possible degradation by-products as well as the toxicity of the effluents. The service life of samples should also be precisely defined as well as the conduction of a complete cost estimation for this kind of systems for commercialization, which is still necessary.

Supplementary Information The online version contains supplementary material available at https://doi.org/10.1007/s11356-024-32467-y.

Acknowledgements The authors gratefully acknowledge RSPU facilities numbers: GS 01/01, GS01/05, GS 02/01, and GS 03/01. The Nanoscopy Science Centre is also gratefully acknowledged for the TEM images. The precious help of dr. F. Fossati and dr. B. Benedetti in the development of the d-Optimal procedure is deeply acknowledged.

Author contribution *Conceptualization*: Mohamed O. Amin, Stefano Alberti; *methodology*: Mohamed O. Amin, Stefano Alberti; *formal analysis and investigation*: Nicolò Ghibaudo, Mohamed O. Amin, Stefano Alberti; *writing — original draft preparation*: Nicolò Ghibaudo, Mohamed O. Amin, Stefano Alberti; *writing — review and editing*: Nicolò Ghibaudo, Maurizio Ferretti, Entesar Al-Hetlani, Metwally Madkour, Mohamed O. Amin, Stefano Alberti; *resources*: Maurizio Ferretti; *Supervision*: Stefano Alberti; *data curation*: Nicolò Ghibaudo, Maurizio Ferretti, Entesar Al-Hetlani, Metwally Madkour, Mohamed O. Amin, Stefano Alberti; *project administration*: Mohamed O. Amin, Stefano Alberti.

Funding Open access funding provided by Università degli Studi di Genova within the CRUI-CARE Agreement.

Data Availability Data available on request from the authors.

Declarations

Ethical approval Not applicable.

Consent to participate Not applicable.

Consent for publication Not applicable.

Competing interests The authors declare no competing interests.

References

Abdulrazaq Y, Abdulsalam A, Larayetan Rotimi A, Aliyu Abdulbasit A, Clifford O, Abdulazeez Abdulsalam O, Nayo Racheal O, Akor Joy A, Omale Victor F, Mbese Johannes Z, Bilal M, Umar MS (2021) Classification, potential routes and risk of emerging pollutants/contaminant, in: Nuro, A. (Ed.), Emerging contaminants. IntechOpen. https://doi.org/10.5772/intechopen.94447

Ahmed S, Khan FSA, Mubarak NM, Khalid M, Tan YH, Mazari SA, Karri RR, Abdullah EC (2021) Emerging pollutants and their removal using visible-light responsive photocatalysis – a comprehensive review. J Environ Chem Eng 9:106643. https://doi.org/10.1016/j.jece.2021.106643

Alberti S, Ferretti M, Vicini S, Castellano M, Caratto V (2019) Porous polydimethylsiloxane membranes loaded with low-temperature crystallized TiO2 NPs for detachable antibacterial films. J Mater Sci 54:1665–1676. https://doi.org/10.1007/s10853-018-2881-4

Alberti S, Basciu I, Vocciante M, Ferretti M (2021a) Experimental and physico-chemical comparison of ZnO nanoparticles' activity for photocatalytic applications in wastewater treatment. Catalysts 11:678. https://doi.org/10.3390/catal11060678

Alberti S, Dodero A, Sartori E, Vicini S, Ferretti M, Castellano M (2021b) Composite water-borne polyurethane nanofibrous electrospun membranes with photocatalytic properties. ACS Appl Polym Mater 3:6157–6166. https://doi.org/10.1021/acsapm.1c01029

Alberti S, Sotiropoulou M, Fernández E, Solomou N, Ferretti M, Psillakis E (2021c) UV-254 degradation of nicotine in natural waters and leachates produced from cigarette butts and heat-not-burn tobacco products. Environ Res 194:110695. https://doi.org/10.1016/j.envres.2020.110695

Alberti S, Rucco M, Di Carro M, Magi E, Ferretti M, Benedetti B (2023) A multidisciplinary approach to the environmental problem of emerging pollution: synthesis and application of a novel composite photocatalyst and the case study of salbutamol degradation. J Environ Chem Eng 11:110262. https://doi.org/10.1016/j.jece.2023.110262

Al-Hetlani E, Amin MO, Madkour M (2017) Detachable photocatalysts of anatase TiO 2 nanoparticles:annulling surface charge for immediate photocatalyst separation. Appl Surf Sci 411:355–362. https://doi.org/10.1016/j.apsusc.2017.03.151

Antonopoulou M, Kosma C, Albanis T, Konstantinou I (2021) An overview of homogeneous and heterogeneous photocatalysis applications for the removal of pharmaceutical compounds from real or synthetic hospital wastewaters under lab or pilot scale. Sci Total Environ 765:144163. https://doi.org/10.1016/j.scitotenv.2020.144163

Azeez F, Al-Hetlani E, Arafa M, Abdelmonem Y, Nazeer AA, Amin MO, Madkour M (2018) The effect of surface charge on photocatalytic degradation of methylene blue dye using chargeable titania nanoparticles. Sci Rep 8:7104. https://doi.org/10.1038/s41598-018-25673-5

Ba-Abbad MM, Takriff MS, Kadhum AAH, Mohamad AB, Benamor A, Mohammad AW (2017) Solar photocatalytic degradation of 2-chlorophenol with ZnO nanoparticles: optimisation with D-optimal design and study of intermediate mechanisms. Environ Sci Pollut Res 24:2804–2819. https://doi.org/10.1007/s11356-016-8033-y

Benedetti B, Tronconi A, Turrini F, Di Carro M, Donno D, Beccaro GL, Boggia R, Magi E (2023) Determination of polycyclic aromatic hydrocarbons in bud-derived supplements by magnetic molecular imprinted microparticles and GC-MS: D-optimal design for a fast method optimization. Sci Rep 13:17544. https://doi.org/10.1038/s41598-023-44398-8

Bhatkhande DS, Pangarkar VG, Beenackers AA (2002) Photocatalytic degradation for environmental applications - a review. J Chem Technol Biotechnol 77:102–116. https://doi.org/10.1002/jctb.532

Boutra B, Sebti A, Trari M (2022) Response surface methodology and artificial neural network for optimization and modeling the photodegradation of organic pollutants in water. Int J Environ Sci Technol 19:11263–11278. https://doi.org/10.1007/s13762-021-03875-1

Chaubey J, Jain V, Singh SK, Jain A, Arora H (2023) Assessment of solar photocatalytic degradation of textile wastewater by ZnO-based reactors. Water Pract Technol 18:2114–2122. https://doi.org/10.2166/wpt.2023.141

Deng Y, Zhao R (2015) Advanced oxidation processes (AOPs) in wastewater treatment. Curr Pollution Rep 1:167–176. https://doi.org/10.1007/s40726-015-0015-z

Deriase SF, El-Salamony RA, Amdeha E, Al-Sabagh AM (2021) Statistical optimization of photocatalytic degradation process of methylene blue dye by SnO – TiO $_2$ – AC composite using response surface methodology. Environ Prog Sustain Energy 40. https://doi.org/10.1002/ep.13639

Dulio V, van Bavel B, Brorström-Lundén E, Harmsen J, Hollender J, Schlabach M, Slobodnik J, Thomas K, Koschorreck J (2018) Emerging pollutants in the EU: 10 years of NORMAN in support of environmental policies and regulations. Environ Sci Eur 30:5. https://doi.org/10.1186/s12302-018-0135-3

González-Pereyra D, González-Rodríguez LM, Villanueva-Rodríguez M, Alonso-Segura D, Aba-Guevara CG, Sanjuan-Galindo R, Ramos-Delgado NA (2022) Dye degradation by heterogeneous and homogeneous photocatalysis processes. A scaled-up approach for a CPC solar reactor. Top Catal 65:1062–1070. https://doi.org/10.1007/s11244-022-01692-5

Grbić B, Radić N, Stojadinović S, Vasilić R, Dohčević-Mitrović Z, Šaponjić Z, Stefanov P (2014) TiO 2 /WO 3 photocatalytic composite coatings prepared by spray pyrolysis. Surf Coat Technol 258:763–771. https://doi.org/10.1016/j.surfcoat.2014.07.082

Grčić I, Radetić L, Miklec K, Presečki I, Leskovar K, Meaški H, Čizmić M, Brnardić I (2024) Solar photocatalysis application in UWWTP outlets - simulations based on predictive models in flat-plate reactors and pollutant degradation studies with in silico toxicity assessment. J Hazard Mater 461:132589. https://doi.org/10.1016/j.jhazmat.2023.132589

Koumaki E, Mamais D, Noutsopoulos C, Nika M-C, Bletsou AA, Thomaidis NS, Eftaxias A, Stratogianni G (2015) Degradation of emerging contaminants from water under natural sunlight: the effect of season, pH, humic acids and nitrate and identification of photodegradation by-products. Chemosphere 138:675–681. https://doi.org/10.1016/j.chemosphere.2015.07.033

Kuspanov Z, Bakbolat B, Baimenov A, Issadykov A, Yeleuov M, Daulbayev C (2023) Photocatalysts for a sustainable future: Innovations in large-scale environmental and energy applications. Sci Total Environ 885:163914. https://doi.org/10.1016/j.scitotenv.2023.163914

Leardi R, Melzi C, Polotti G (2019) CAT (Chemometric Agile Tool), freely downloadable from http://gruppochemiometria.it/index.php/software

Liu Y, Zhu Q, Tayyab M, Zhou L, Lei J, Zhang J (2021) Single-atom Pt loaded zinc vacancies ZnO–ZnS induced type-V electron transport

for efficiency photocatalytic H_2 evolution. Solar RRL 5:2100536. https://doi.org/10.1002/solr.202100536

Luna-Sanguino G, Ruíz-Delgado A, Tolosana-Moranchel A, Pascual L, Malato S, Bahamonde A, Faraldos M (2020) Solar photocatalytic degradation of pesticides over TiO2-rGO nanocomposites at pilot plant scale. Sci Total Environ 737:140286. https://doi.org/10.1016/j.scitotenv.2020.140286

Martinelli A, Alberti S, Caratto V, Lova P, Locardi F, Pampararo G, Villa S, Ferretti M (2018) Structural studies on copper and nitrogen doped nanosized anatase. Z Kristallogr – Cryst Mater 233:867–876. https://doi.org/10.1515/zkri-2017-2143

Merino-Mantilla MJ, Salinas-Brigante CA, Quinones-Murillo DH (2019) Design and evaluation of a reactor prototype for the removal of emerging contaminants from industrial sewage through solar-driven photocatalysis and ozonation, in: 2019 7th International Engineering, Sciences and Technology Conference (IESTEC). Presented at the 2019 7th International Engineering, Sciences and Technology Conference (IESTEC), IEEE, Panama, Panama, pp 237–242. https://doi.org/10.1109/IESTEC46403.2019.00-69

Mustafa YA, Al-Jobouri HA, Jaid KM (2023) Solar photocatalytic degradation of diuron in aqueous solution by TiO2. Jcoeng 20:80–90. https://doi.org/10.31026/j.eng.2014.11.06

Pal A, Gin KY-H, Lin AY-C, Reinhard M (2010) Impacts of emerging organic contaminants on freshwater resources: review of recent occurrences, sources, fate and effects. Sci Total Environ 408:6062–6069. https://doi.org/10.1016/j.scitotenv.2010.09.026

Rapti I, Kosma C, Albanis T, Konstantinou I (2023) Solar photocatalytic degradation of inherent pharmaceutical residues in real hospital WWTP effluents using titanium dioxide on a CPC pilot scale reactor. Catal Today 423:113884. https://doi.org/10.1016/j.cattod.2022.08.026

Ribeiro AR, Pedrosa M, Moreira NFF, Pereira MFR, Silva AMT (2015) Environmental friendly method for urban wastewater monitoring of micropollutants defined in the Directive 2013/39/EU and Decision 2015/495/EU. J Chromatogr A 1418:140–149. https://doi.org/10.1016/j.chroma.2015.09.057

Rueda-Marquez JJ, Levchuk I, Fernández Ibañez P, Sillanpää M (2020) A critical review on application of photocatalysis for toxicity reduction of real wastewaters. J Clean Prod 258:120694. https://doi.org/10.1016/j.jclepro.2020.120694

Rykowska I, Wasiak W (2015) Research trends on emerging environment pollutants – a review. Open Chem 13:000010151520150151. https://doi.org/10.1515/chem-2015-0151

Sivaraman C, Vijayalakshmi S, Leonard E, Sagadevan S, Jambulingam R (2022) Current developments in the effective removal of environmental pollutants through photocatalytic degradation using nanomaterials. Catalysts 12:544. https://doi.org/10.3390/catal12050544

Sousa MA, Gonçalves C, Vilar VJP, Boaventura RAR, Alpendurada MF (2012) Suspended TiO2-assisted photocatalytic degradation of emerging contaminants in a municipal WWTP effluent using a solar pilot plant with CPCs. Chem Eng J 198–199:301–309. https://doi.org/10.1016/j.cej.2012.05.060

Sousa JCG, Ribeiro AR, Barbosa MO, Pereira MFR, Silva AMT (2018) A review on environmental monitoring of water organic pollutants identified by EU guidelines. J Hazard Mater 344:146–162. https://doi.org/10.1016/j.jhazmat.2017.09.058

Tayyab M, Liu Y, Liu Z, Pan L, Xu Z, Yue W, Zhou L, Lei J, Zhang J (2022) One-pot in-situ hydrothermal synthesis of ternary In2S3/Nb2O5/Nb2C Schottky/S-scheme integrated heterojunction for efficient photocatalytic hydrogen production. J Colloid Interface Sci 628:500–512. https://doi.org/10.1016/j.jcis.2022.08.071

Tayyab M, Liu Y, Liu Z, Xu Z, Yue W, Zhou L, Lei J, Zhang J (2023) A new breakthrough in photocatalytic hydrogen evolution by amorphous and chalcogenide enriched cocatalysts. Chem Eng J 455:140601. https://doi.org/10.1016/j.cej.2022.140601

Tayyab M, Kulsoom UE, Liu Y, Mansoor S, Khan M, Akmal Z, Mushtaq A, Arif M, Shamriaz U, Zhou L, Lei J, Zhang J (2024) Visible light-driven photocatalytic H2 evolution and dye degradation by electrostatic self-assembly of CdS nanowires on Nb2C MXene. Int J Hydrogen Energy 51:1400–1413. https://doi.org/10.1016/j.ijhydene.2023.09.199

Thommes M, Kaneko K, Neimark AV, Olivier JP, Rodriguez-Reinoso F, Rouquerol J, Sing KSW (2015) Physisorption of gases, with special reference to the evaluation of surface area and pore size distribution (IUPAC Technical Report). Pure Appl Chem 87:1051–1069. https://doi.org/10.1515/pac-2014-1117

Umh HN, Kim Y (2014) Sensitivity of nanoparticles' stability at the point of zero charge (PZC). J Ind Eng Chem 20:3175–3178. https://doi.org/10.1016/j.jiec.2013.11.062

Vasilopoulou M (2014) The effect of surface hydrogenation of metal oxides on the nanomorphology and the charge generation efficiency of polymer blend solar cells. Nanoscale 6:13726–13739. https://doi.org/10.1039/C4NR04408H

Villa S, Caratto V, Locardi F, Alberti S, Sturini M, Speltini A, Maraschi F, Canepa F, Ferretti M (2016) Enhancement of TiO2 NPs activity by Fe3O4 nano-seeds for removal of organic pollutants in water. Materials 9:771. https://doi.org/10.3390/ma9090771

Yang X, Wang D (2018) Photocatalysis: from fundamental principles to materials and applications. ACS Appl Energy Mater 1:6657–6693. https://doi.org/10.1021/acsaem.8b01345

Yang Y, Ok YS, Kim K-H, Kwon EE, Tsang YF (2017) Occurrences and removal of pharmaceuticals and personal care products (PPCPs) in drinking water and water/sewage treatment plants: a review. Sci Total Environ 596–597:303–320. https://doi.org/10.1016/j.scitotenv.2017.04.102

Younis S, Kim K-H (2020) Heterogeneous photocatalysis scalability for environmental remediation: opportunities and challenges. Catalysts 10:1109. https://doi.org/10.3390/catal10101109